Combustion and Flame 234 (2021) 111591

Contents lists available at ScienceDirect

Combustion and Flame

journal homepage: www.elsevier.com/locate/combustflame

Effect of oxygen on the burning rate of wood

Franz Richter[a,b], Freddy X. Jervis[c], Xinyan Huang[d], Guillermo Rein[a,*]

[a] Department of Mechanical Engineering, Imperial College London, United Kingdom
[b] Department of Mechanical Engineering, University of California, Berkeley, United States
[c] Facultad de Ingeniería en Mecánica y Ciencias de la Producción, Escuela Superior Politecnica del Litoral, ESPOL, Guayaquil, Ecuador
[d] Department of Building Services Engineering, Hong Kong Polytechnic University, Hong Kong

ARTICLE INFO

Article history:
Received 1 April 2020
Revised 27 June 2021
Accepted 28 June 2021
Available online 1 October 2021

Keywords:
Timber
Biomass
Fire
Smouldering
Charring

ABSTRACT

The large-scale adoption of wood as a construction material for tall buildings could pave the way for sustainable construction. Its adoption, however, is hindered by a limited understanding of wood's behaviour in a fire. In particular, the effect of oxygen and heat flux on the burning (including pyrolysis) and ignition behaviour of wood is poorly understood. We addressed this gap by studying the effect of oxygen concentration and heat flux on the burning and ignition behaviour of particleboard experimentally and computationally. Particleboard was chosen as a proxy for all woody construction materials. We conducted over 60 experiments in an FPA on samples of particleboard spanning different oxygen concentrations (0–21%), heat fluxes (10–70 kW/m^2), sample densities (600–800 kg/m^2), and sample thicknesses (6–25 mm). Only the heat flux and oxygen concentration significantly affected the charring rate, time-to-flaming ignition, and burning mode (pyrolysis, smouldering, flaming). To explore this effect further, we used a multi-physics model of particleboard charring developed in Gpyro. Combining the computational and experimental results, we showed that particleboard undergoes only pyrolysis in oxygen concentrations below 4%, smouldering between 4 and 15%, and flaming above 15% at a heat flux of 30 kW/m^2. These oxygen concentration thresholds were found to decrease as the heat flux increases. We also showed that smouldering and flaming increases the charring rate by 25 and 37%, respectively. This means that the rate of loss of a section of structural wood, quantified by the charring rate, in a fire due to smouldering is similar to that of flaming combustion. In addition, we noted the existence of a triple point for the ignition of wood at which a slight change in environmental conditions can lead to either smouldering, flaming, or only pyrolysis. In summary, this paper quantified for the first time the contributions of the three modes of burning to the charring rate of wood and highlights the importance of smouldering for timber construction.

1. Introduction to wood fires

Engineered wood is becoming a popular construction material due to its strength, lightweight, and sustainability [1]. It is made by gluing wood fibres (Medium Density Particleboard), chips (Low-Density Particleboard), or planks (Cross Laminated Timber) together in various assemblies. However, a limited understanding of the fire behaviour of engineered wood hinders its uptake [1]. Specifically for tall buildings, wooden products are largely prohibited or too costly due to the strict fire safety and structural requirements. The fire behaviour of wood is largely dependent on the charring (pyrolysis) and burning behaviour of wood, which controls both the loss of load-bearing section (strength loss) and the production of gaseous and solid fuel needed to estimate heat release rates [40]. We explore the charring and burning behaviour of particleboard as a proxy for engineered woods.

Previous studies have investigated wood at the micro- (mg-samples, usually TGA experiments) and mesoscale (g-samples, usually Cone Calorimeter experiments) [2–5]. They explored the process of pyrolysis [3,6], cracking [7], flaming ignition [8], and flame spread [4]. However, these studies did not address the full charring and burning behaviours of wood, as they considered only a single oxygen concentration. The charring and burning behaviour of any polymer–wood is a natural polymer and represents over 90 % of the mass of particleboards– depends on the oxygen concentration of the surrounding atmosphere [8]. Current studies on flame spread and ignition of fibreboard [4,9]—the closest studied material in the literature to particleboard—have focused on the charring and burning behaviour in air, where flaming ignition occurs within a few minutes at heat flux levels greater than 12 kW/m^2 [8]. However, some studies of the fire resistance of structural wood are

* Corresponding author.
E-mail address: g.rein@imperial.ac.uk (G. Rein).

https://doi.org/10.1016/j.combustflame.2021.111591
0010-2180/

Nomenclature

A	pre-exponential factor (1/s)
c	heat capacity (J/kg-K)
E	activation energy (J/mol)
h	enthalpy (J)
h_c	convective coefficient (W/m^{2}s)
h_m	mass transfer coefficient (kg/m^2-s)
ΔH	heat of reaction (kJ/mol)
k	thermal conductivity (kg/m^3)
K	permeability (m^2)
$\dot{m}''$	mass flux (g/m^2-s)
n	heterogeneous reaction order (-)
P	pressure (Pa)
$\dot{q}''$	heat flux (kW/m^2)
R	universal gas constant (J/mol-k)
t	time (s)
T	temperature (°C)
Y	mass fraction (g/g)
z	distance (mm)
n_{O_2}	oxygen reaction order (-)
$[O_2]_a$	ambient oxygen concentration (%)
$[O_2]_s$	surface oxygen concentration (%)

Greeks

ε	emissivity (-)
ρ	bulk density (kg/m^3)
ν	Viscosity (m^2/s)/stoichiometry or solid yield
ρ_{so}	solid density, ρ/ρ_s=1-Φ
Φ	porosity (-)
$\dot{\omega}'''$	volumetric reaction rate (kg/m^3-s)

Subscripts

0	Initial
g	gas
i	condensed species number
j	gaseous species number
k	reaction number
O_2	local oxygen
aO_2	ambient oxygen

conducted in furnaces where the oxygen concentration near the sample surface is below 8% [10]. Flaming would not be expected to take place at oxygen concentrations below 8 %, as it is outside the lower flammability limit of the volatiles. A polymer would be expected to undergo pyrolysis or smouldering at these conditions[11–13]. A real compartment fire could involve regions with different oxygen levels and heat fluxes, which all have to be considered to accurately capture the structural behaviour of woody materials.

Smouldering is the low temperature and flameless heterogeneous combustion of solids [11,12]. In the absence of oxygen, a polymer will undergo pyrolysis without any oxidation. In the presence of oxygen, a polymer will undergo pyrolysis together with oxidation. If the solid product from pyrolysis, called char, oxidises, the mode of burning is called smouldering. If the gaseous products from pyrolysis, called volatiles, oxidise, the mode of burning is called flaming. Both smouldering and flaming can be present simultaneously. Notably, we will also refer henceforth to the process of pyrolysis as a mode of burning, despite it involving no oxidation. This choice was made for simplicity as pyrolysis is a predecessor for combustion.

Different oxygen concentrations are expected to give rise to different modes of burning (Fig. 1). Each of these modes presents a unique fire or structural hazard. For example, a flaming fire propagates faster but is easier to extinguish than a smouldering fire.

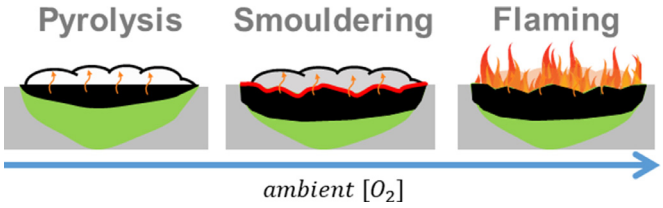

Fig. 1. Three modes of burning (pyrolysis, smouldering, flaming) as a function of ambient oxygen concentration. Pyrolysis supplies the fuel for smouldering and flaming and is the first step in the charring of wood. Flaming and smouldering both have the potential to transition from one another.

Any of these modes (pyrolysis, smouldering, flaming) can transition to one another [12]. In building fires, the oxygen concentration varies across the compartment, and all modes are expected to take place. This fluctuation makes it important to understand each mode and the transitions between them. Although several papers studied the critical heat flux for flaming and smouldering extinction of wood [14,15,47], to date, few studies have investigated the critical conditions (especially oxygen concentration) for the ignition of smouldering and transition between the modes [11,16–19]. Few of these studies have quantified the relative contribution of each mode, which is a necessary step to unravel the transition between the modes [20]. In this study, we aim to understand the effect of oxygen concentration and heat flux on the charring and burning behaviour of particleboard.

2. Experimental and computational method

2.1. Experimental method

The experiments were conducted using a Fire Propagation Apparatus (FPA) following the ASTM E 2058 standard. In an FPA, the fuel sample is exposed to a radiative heat flux, and a pilot ignition source placed above its free surface. In this study, the range of radiative heat imposed varied from 10 to 70 kW/m^2 and was maintained constant for the whole duration of the experiment. The sample mass was continuously measured and the exhaust gases were analysed for composition, temperature, and flow rate. The ambient conditions were controlled through an imposed gas flow of varying oxygen concentrations ranging from 0 to 21%. The flow speed was set to 200 l/min, which is recommended by the manufacture and ASTM E 2028 to avoid the effects of oxygen depletion inside the FPA.

The sample size studied was 8 by 8 cm with different thicknesses. The sides and back of the sample were wrapped by three layers of cotronics ceramic paper (each 3 mm thick) to minimise heat losses. The top of the sample was exposed to a constant heat flux. The sample was then pushed into a metallic holder and placed on the mass balance. The Heat Release Rate was obtained through the carbon dioxide and carbon monoxide generation method, as discussed in [21]. The mass flux was obtained by differentiating and smoothing the measured mass over time. Table S1 lists our 69 experiments of particleboard with different densities, thicknesses, heat fluxes, and oxygen concentrations.

2.2. Computational model formulation, mesh, and input parameters

We developed a generalised pyrolysis model of particleboard in Gpyro [22] consisting of chemical kinetics and transport submodels. These two are the most important processes that affect the charring of wood, as shown in Fig. 3. The process of cracking and delamination are not considered because particleboards are not laminated (does not delaminate) and cracking was not

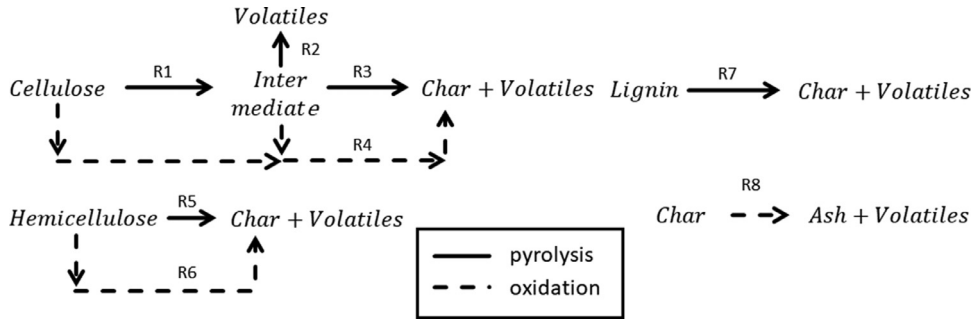

Fig. 2. Sketch of reaction scheme from [24].

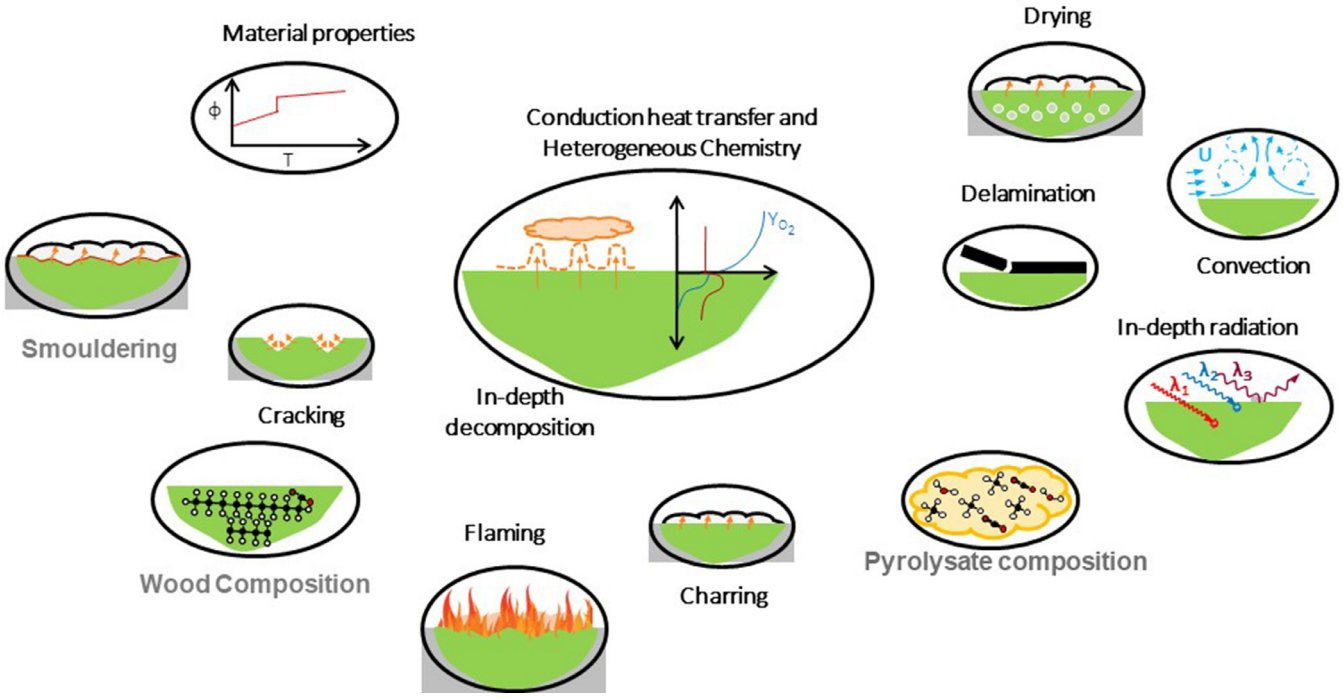

Fig. 3. Sketch of the different chemical, physical, and mechanical processes that affect the charring rate of timber. The process of cracking and delamination are not considered here, as we particleboards are non-laminated (does not delaminate), and cracking was not found significant in our experiments.

found significant in our experiments. This model has been validated at three scales: micro-, meso-, and macroscale. At the microscale, it was validated with over 80 TGA experiments [23]. At the mesoscale, it was validated with Cone Calorimeter experiments, where it predicted the pyrolysis and smouldering behaviour (pyrolysis + smouldering, but no flaming) of different wood species under different heat fluxes, oxygen concentrations, and different grain directions [24]. At the macroscale, the model was validated with standard furnaces tests [25].

The chemical kinetics, both reaction scheme and kinetic parameters, of wood, were taken from [23], with the reaction scheme shown in Fig. 2.

The consumed oxygen for pyrolysis reactions (R1-R3,R5,R7) is 0, for fuel oxidation (R4 & R6) reactions it is 0.41 g/g-fuel [26], and for char oxidation (R8) reactions it is six times the amount of fuel oxidation (2.46 g/g-fuel) [27]. The heats of reaction are taken from [23,26,28]. The reaction scheme is the linear superposition of the three main components of wood: cellulose, hemicellulose, and lignin. It consists of five pyrolysis reactions, two fuel oxidation reactions, one char oxidation reaction, and six solid species (cellulose, hemicellulose, lignin, intermediate, char, and ash). The respective initial mass fractions of cellulose, hemicellulose, and lignin is assumed fixed at 0.459, 0.251, and 0.29 respectively [29]. The measured moisture content was around 5%, which was deemed insufficient to include a drying model.

The rate of pyrolysis and oxidation reactions can be described by Eq. (1)

$$\dot{\omega}_i''' = \bar{\rho} Y_{A,k} Y_{O_2}^{n_{O_2,k}} A_k \exp\left(-E_k/RT\right) \tag{1}$$

This kinetic model is incorporated into Gpyro, which solves the main five one-dimensional conservation equations for condensed-phase mass (2), species (3), and energy (4), and those for the gas-phase mass (5), species (6), and momentum (7):

$$\frac{\partial \bar{\rho}}{\partial t} = -\dot{\omega}_{fg}''' \tag{2}$$

$$\frac{\partial (\bar{\rho} Y_i)}{\partial t} = \dot{\omega}_{fi}''' - \dot{\omega}_{di}''' \tag{3}$$

$$\frac{\partial \left(\bar{\rho}\bar{h}\right)}{\partial t} = k \frac{\partial}{\partial z}\left(\frac{\partial T}{\partial z}\right) + \dot{\omega}_{fi}'''(-\Delta H_i) \tag{4}$$

$$\frac{\partial}{\partial t}\left(\rho_g \bar{\phi}\right) + \frac{\partial \dot{m}''}{\partial z} = \dot{\omega}_{fg}''' \tag{5}$$

Table 1
Material properties used in this study. Quantities denoted with the sign # indicate calculations and * indicate measurements.

Species (i)	ρ_i (kg/m^3)	k_i (kg/m^3)	c_i (J/kg-K)	ε (-)	γ (mm)	ρ_{soi} (kg/m^3)	K x 10^{10} (m^2)	d_p (mm)
Timber	630*	0.189 [2]	2300 [5]	0.7 [31]	0.612#	1513 [32]	0.01#	0.03#
Char	220#	0.117 [2]	1100 [5]	0.95 [5]	1.29#	1467 [5]	0.083#	0.09#
Ash	18.9#	0.8 [33]	880 [33]	0.95 [33]	3.76#	2500 [33]	0.7#	2.65#

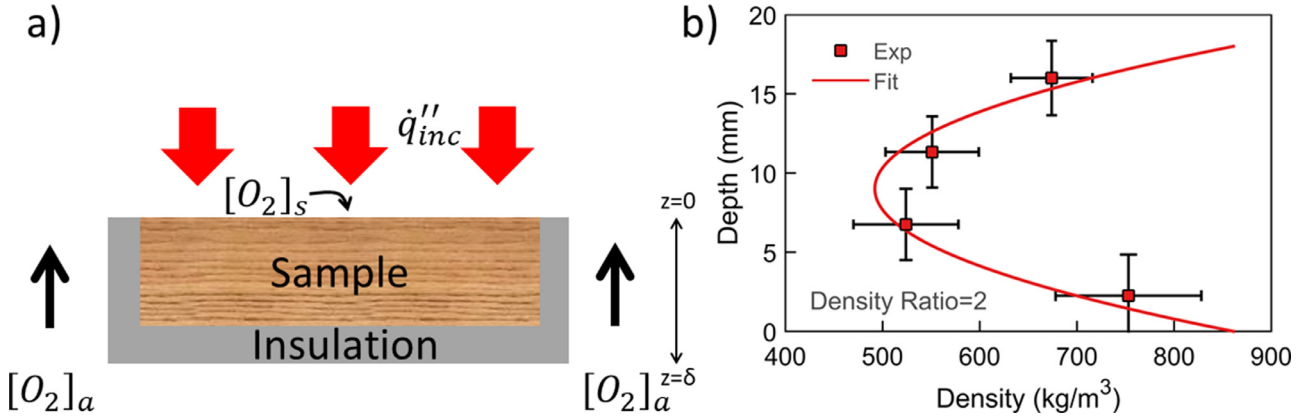

Fig. 4. a) Sketch of oxygen flow and irradiation to the sample in the experimental appartus. b) Comparison between measured and fitted density profile of the particleboard.

$$\frac{\partial}{\partial t}\left(\rho_g \bar{\phi} Y_j\right) + \frac{\partial}{\partial z}\left(\dot{m}'' Y_j\right) = -\frac{\partial}{\partial z}\left(\bar{\phi}\rho_g D \frac{\partial Y_j}{\partial z}\right) + \dot{\omega}'''_{fj} - \dot{\omega}'''_{dj} \tag{6}$$

$$\dot{m}'' = -\frac{\kappa}{\nu}\frac{\partial p}{\partial z} \tag{7}$$

The overbar represents the respective mass or volume average. The mesh size was 0.1 mm, and the time step was 0.1 s. All material properties were taken from the literature and given in Table 1. The pore diameter d_p was calculated from the density [30], the permeability was calculated from the pore diameter [30], and the radiative conductivity component was calculated from the emissivity and pore diameter [2].

2.3. Boundary condition

The boundaries of the sample consist of a free surface at $z = 0$ and an insulated surface $z = \delta$, as shown in Fig. 4a. At the back surface ($z = \delta$), we assume that the surface is adiabatic ($h = 0$) and impermeable ($\frac{dP}{dt} = 0$). At the front surface ($z = 0$). we assume $h =$ 10 W/m^2-s [9] and a mass transfer coefficient of $h_m = 0.01$ kg/m^2-s. The heat flux at z = 0 is defined in Eq. (8):

$$\dot{q}''_{inc} = \begin{cases} \dot{q}_{ir}, & [O_2]_a < 15\% \\ \dot{q}_{ir} + \dot{q}_f, & [O_2]_a > 15\% \quad t_{ig} < t < t_{fl} \end{cases} \tag{8}$$

where $\dot{q}_{ir}$ is the irradiation from the heater, $\dot{q}_f$ the flaming heat flux, and $\dot{q}_{inc}$ the incident heat flux on the sample surface. The flaming heat flux is fitted based on experimental measurement, as $\dot{q}_f = 137 Y_{aO_2}^{1.3}$, where Y_{aO_2} is the ambient oxygen mass fraction. Y_{aO_2} is calculated from $[O_2]_a$ assuming the split of oxygen and nitrogen at standard conditions in air. This flaming heat flux correlation is based on [34] and a flaming heat flux of 20 kW/m^2 in air [9]. Note that the flaming heat flux has a growth period of 70 s and a decay period in the last 170 s before extinction (Fig. 5), according to the experiment in [9]. Notably, particleboard shows a parabolic non-uniform density profile, which is defined based on the medium density and ratio of maximum to minimum density ($\rho_{\max}/\ \rho_{\min}$) in the sample [6]. For particleboard, we measured that density ratio to be two by measuring the density of individual slices of different depths (Fig. 4b). Such a parabolic shape was modelled in Gpyro by 18 discrete density layers [9].

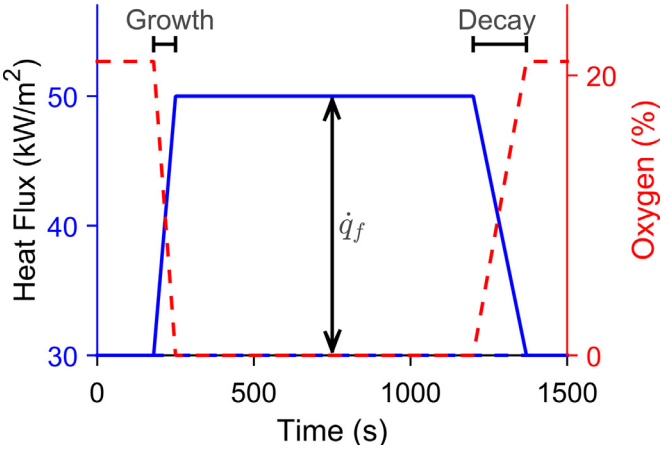

Fig. 5. Sketch of the time evolution of the applied heat flux and oxygen concentration at the surface of a sample under constant irradiation of 30 kW/m^2 from the FPAand 21% ambient oxygen.

In Eq. (1), the local oxygen mass fraction Y_{O_2} is used to calculate the reaction rate. Y_{O_2} is determined via Eq. (6) using the oxygen fraction of the sample surface and the mass transfer coefficient as a boundary condition. Due to the presence of a flame, the oxygen concentration at the surface differs from the ambient oxygen concentration and is calculated in Eq. (9). Notably, the oxygen mass fraction is used in Gpyro instead of the oxygen concentration.

$$[O_2]_s = \begin{cases} [O_2]_a, & [O_2]_a < 15\% \\ f(\mathrm{CR}), & [O_2]_a > 15\% \end{cases} \tag{9}$$

The function $f(CR)$ is calculated in Eq (10).

$$[O_2]_s = f(\mathrm{CR}) = \frac{\mathrm{CR}([O_2]_a) - \mathrm{CR}_{\min}}{\mathrm{CR}_{max} - \mathrm{CR}_{min}}\ [O_2]_a \tag{10}$$

where CR stands for carbon ratio, $\mathrm{CR}([O_2]_a)$ is a spline fit to the measured CO/CO_2 ratios evaluated at $[O_2]_a$, CR_{min} is the minimum measured CO/CO_2 ratio for smouldering without flame, and CR_{max}

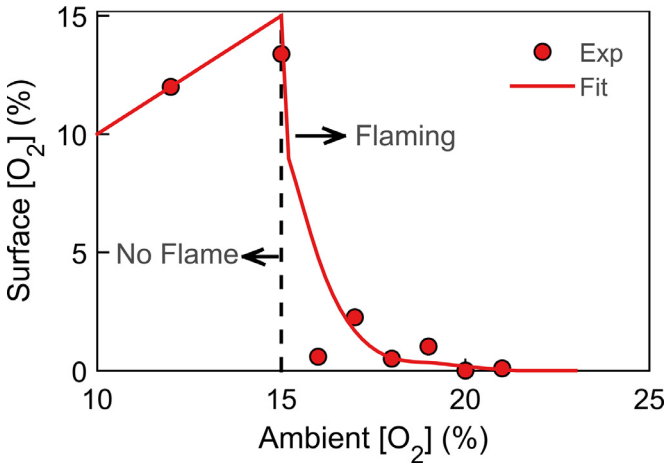

Fig. 6. Dependence of surface oxygen concentration on ambient oxygen concentration with a criticality at 15% for flaming.

is the maximum measured CO/CO_2 ratio for a strong flame. A comparison between the predictions of $[O_2]_s$ with Eq. (10) and experimental data is illustrated in Fig. 6. Good agreement was observed across all oxygen concentrations.

In other words, we know for certain that below 15% $[O_2]_a$ we have no flame and only smouldering is present and that at 21% $[O_2]_a$ we only have flaming present. At $15<[O_2]_a<21\%$, both could be present. The flaming to the incident heat flux is calculated by interpolation, which is analogous to the concept of the modified combustion efficiency (MCE) that has been previously used to assess the relative contribution of flaming and smouldering during the charring of solids [35]. The idea of the MCE is that the lower the value, the larger the amount of CO released, the more incomplete the combustion, and hence, the weaker the flame. This idea was used in Eq. (10) to estimate the amount of oxygen arriving at the solid's surface in the presence of a flame, as a stronger flame is expected to consume more oxygen and release less CO than a weaker flame. Notably, we took CR_{min} at 12% $[O_2]_a$, as some studies reported flaming at around 15% [16,17], and we wanted to choose a value of CR_{min} away from the transition point between flaming and smouldering. Choosing the CR_{min} at 15% would result in an 8% change in CR_{min} value. Furthermore, the above was expressed in CR instead of MCE (=1/(1+CR)) as we found better agreement using CR than MCE with the experimental data. MCE predicts a higher $[O_2]_a$ than CR. Fig. 6 compares the experimentally measured values of the surface oxygen concentrations with those calculated by Eq. (10). The line was fitted using the fit function in Matlab with a highly smooth spline. In addition, the rate of supply of oxygen from the ambient to the surface exceeds the rate of consumption of oxygen by smouldering, so that the concentration of oxygen at the surface is constantly around the ambient value in the absence of a flame.

3. Results and discussion

3.1. Model validation and analysis

The model was developed at the microscale and mesoscale against several experiments based on our previous work on natural wood [23,29]. Engineered wood differs from natural wood due to the presence of resin (affects kinetic model and heat of reactions), absence of grain direction (thermal conductivity), density gradient (density), and porosity gradient (porosity, pore diameter). We found the resin to have an insignificant influence on the chemical kinetics as our chosen kinetic model performs well against the experiments of MDF [9], the closest related material studied in the literature the microscale (error = $1.1\sigma_e$ in mass loss history). At the mesoscale, we further found that the heat of reactions and coefficient of oxygen consumption of natural wood perform well for particleboard as well. This conclusion was drawn from a sensitivity study and comparison with the experiments of 18 mm particleboard at 0 and 12% (Fig. 7a & b, error = $1.05\ \sigma_e$). Following the sensitivity analysis, the heat of reaction of the fuel oxidation of hemicellulose (R6) was set to zero due to its insignificant influence across the whole literature range. We accounted for the absence of grain direction in particleboard by using a thermal conductivity of wood and char that resembles the average thermal conductivity ($k = 0.189$ W/m − K) [36] of wood across all three grain directions ($k \approx 0.2$ W/m − K) [2].

Particleboard is known to have a density gradient, which was measured in Section 2.3. A density gradient implies a porosity and permeability gradient. We accounted for this effect by making the porosity ($\phi = 1 - \rho/\rho_{s0}$) of particleboard dependant on the bulk density (ρ) through a constant solid density (ρ_s). That is, the pore diameter is a function of the bulk density, and the permeability is a function of the pore diameter. A sensitivity study revealed that the model is insensitive to the exact value of these parameters, while a comparison with experiments (Fig. 8, Fig S1 for rotated form) showed good agreement (error = $1.16\sigma_e$). The largest errors, up to $6.3\sigma_e$, are observed at low heat fluxes (below 20 kW/m^2). Thus, the model is suitable to investigate the fundamental processes of charring particleboard.

3.2. Mass loss rate and limiting oxygen concentration

Modelling results revealed that the oxygen concentration controls the mode of burning for particleboard. At 30 kW/m^2, pyrolysis dominates below 4% $[O_2]_a$, while smouldering dominates between 4% and 15% $[O_2]_a$, and flaming dominates above 15% $[O_2]_a$. Fig. 9 compares the predicted average mass loss rate with the measured average mass loss rate, where predictions are within the experimental uncertainty, showing an excellent agreement. It is well established in the literature that there are three modes of burning (pyrolysis, smouldering, and flaming) for any charring material, which are significantly influenced by the oxygen concentration [11]. Pyrolysis is the thermal degradation of biomass that does not require oxygen. Smouldering is the low-temperature heterogeneous combustion of biomass [37]. Within this study, we defined the boundary of smouldering by the threshold of a propagating char oxidation reaction. Flaming is the homogeneous combustion of volatiles.

Based on our model predictions, we found that below 4% $[O_2]_a$, only pyrolysis and fuel oxidation reactions take place. The oxidation of char is restricted to the surface and cannot form a propagation. We concluded that charring is controlled by pyrolysis under these conditions. Only at above 4% $[O_2]_a$, the oxidation of char becomes significant and starts to travel into the solid. Note that this limiting oxygen concentration will increase as the external radiation decreases. This fact manifests itself in the model through a large uncertainty (red cloud, Fig. 9) that is a result of the uncertainty in the heat of char oxidation. Around 15% $[O_2]_a$, we experimentally observed the appearance of a flame or flashes (Fig. 9), from which we conclude that this is the point of the criticality of flaming under given external radiation (30 kW/m^2). The appearance of a flame coincides with the ceasing of smouldering during the period of flaming (lasting 850 s). Smouldering ceases due to the consumption of oxygen by the flame above the solid, which we also confirmed computationally by seeing no smouldering reaction during the flaming period (Fig S2).

The discovered limiting oxygen concentration of flaming under the external radiation (14–15% for wood) agrees well with the liter-

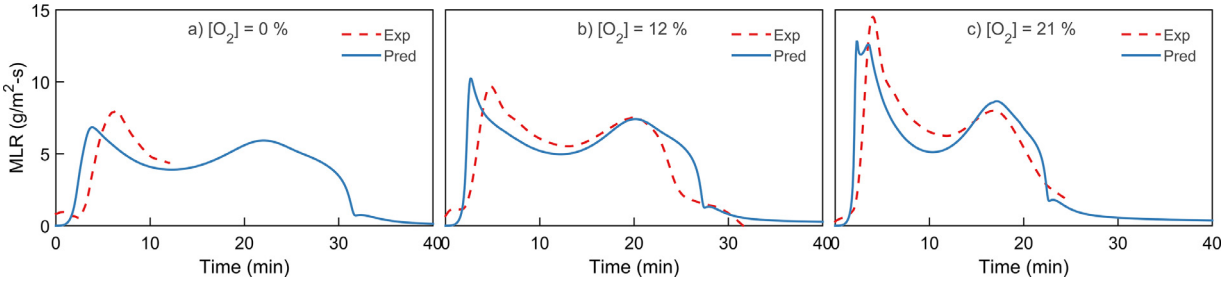

Fig. 7. Comparison between experiments and predictions at three oxygen concentrations at 30 kW/m^2 of an 18 mm thick sample.

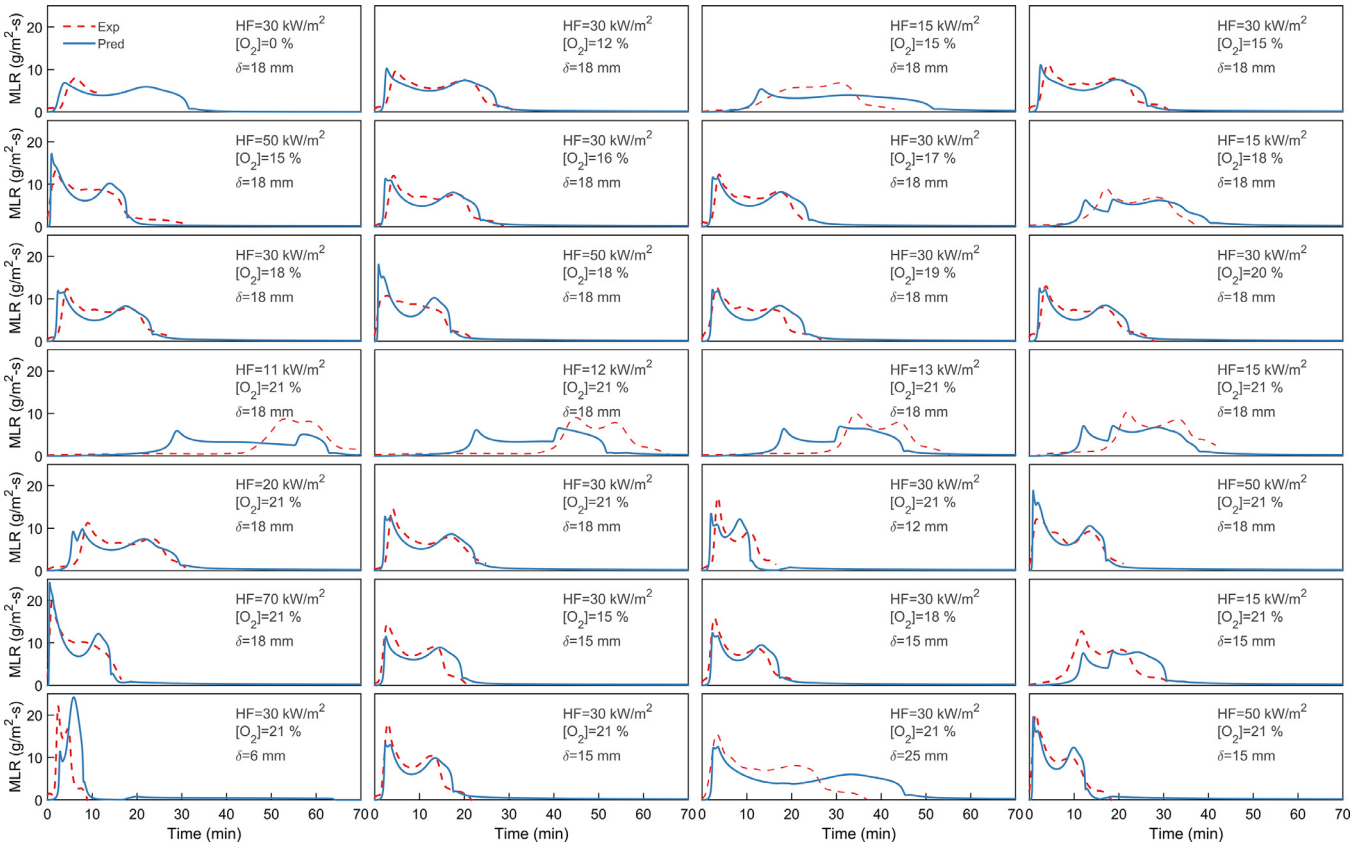

Fig. 8. Comparison between all unique experiments, in terms of conditions, and the prediction.

ature where the PU Foam was found to transition from smouldering to flaming above 17% $[O_2]_a$ [38]. Plastics were found to support sustained flaming above 14–16% $[O_2]_a$ depending on the pressure [34], and external radiation [13]Moss was found to ignite by flaming above 15% $[O_2]_a$ [17]. Similarly, our criticality of smouldering agrees well with the literature where self-sustained smouldering was found to require 10% $[O_2]$ [39], but aided smouldering requires 5% $[O_2]_a$ [19], which is close to our threshold of 4%.

The average mass loss rate in all three modes of burning is of the same magnitude, which means that each mode poses a hazard. For example, the charring rate of particleboard at 20% $[O_2]_a$ is only double that at 10% $[O_2]_a$. For a wood structural component (timber), the fire performance is evaluated by the charring rate (speed of pyrolysis front) [40], which is positively correlated to the mass loss rate. A smouldering timber member would also experience a significant charring rate, comparable to a flaming timber member. This finding could explain the significant strength-loss [40] after flaming has ceased, as observed in fire tests of timber (referred to as the cooling phase) [41]. Wiesner et al. [41] showed that this strength loss during the "cooling" phase of a fire is not incorporated in current fire safety designs and highlighted the subsequent increased risk. Our findings here support the hypothesis that strength loss of timber can be significant in the absence of flaming due to smouldering driven combustion. In fact, the visuals of Kinjo et al. [42] showed a glowing timber beam after a fire test, which indicated a robust smouldering. This evidence provides a case for an increasing need to examine smouldering in more detail for timber structures, as proposed elsewhere [43].

3.3. Ignition thresholds for wood

The charring behaviour of wood is influenced by both oxygen concentration and heat flux. Fig. 10 shows the Ignition Diagram for wood that describes the effect of oxygen and heat flux on the mode of burning. As described in Section 3.2, there are two ignition thresholds for wood: one for smouldering combustion and one for flaming combustion. The limiting oxygen concentration decreases for both of them as the heat flux increases. A similar phenomenon has previously been observed for flame spread over plastics [44] and for the extinction of wood [18]. Comparing our

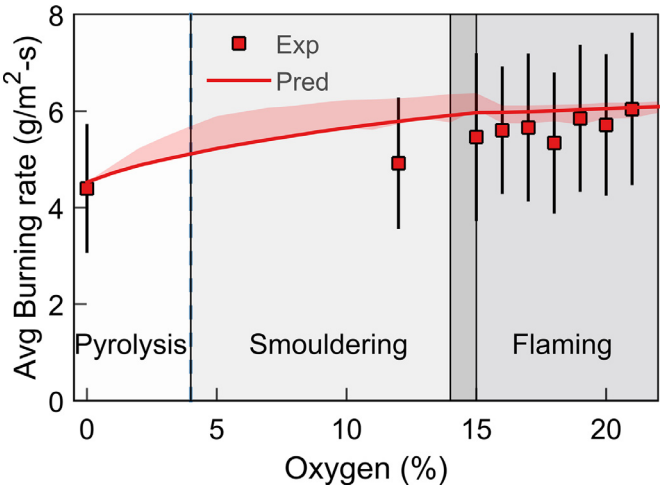

Fig. 9. Average charring rate against oxygen concentration for a low-density particleboard sample of 18 mm at a constant heat flux of 30 kW/m^2 for a time of 1500s (average running time of the experiments). The red cloud represents the model uncertainty.

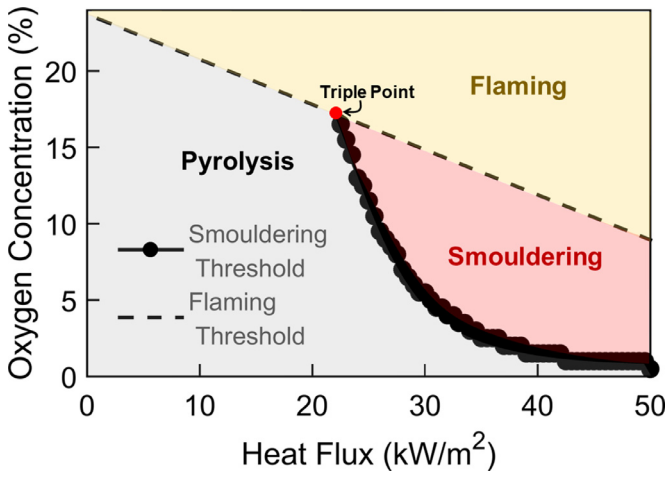

Fig. 10. Influence of oxygen and heat flux on the ignition thresholds for timber. The flaming threshold is based on experimental measurements at 13, 15, and 30 kW/m^2. The smouldering threshold is based on simulations. Notably, the thresholds only hold for ignition.

experimental measurements for the flaming ignition of wood with those for flaming extinction of wood by Cuevas et al. [18] suggests that the threshold for ignition and extinction of wood differ. They found flaming extinction thresholds at 30, 35, and 40 kW/m^2 and an oxygen concentration of 21, 19, and 17%, respectively. We found flaming ignition thresholds at 30, 35, and 40 kW/m^2 and an oxygen concentration of 15, 13, and 12%, respectively. We conclude that our data should only be treated as ignition thresholds for flaming and smouldering from this comparison. They may not hold for extinction.

Our ignition diagram reveals for the first time a triple point for the ignition of wood at a heat flux of 22 kW/m^2 and an oxygen concentration of 17%. The exact value of the triple point is

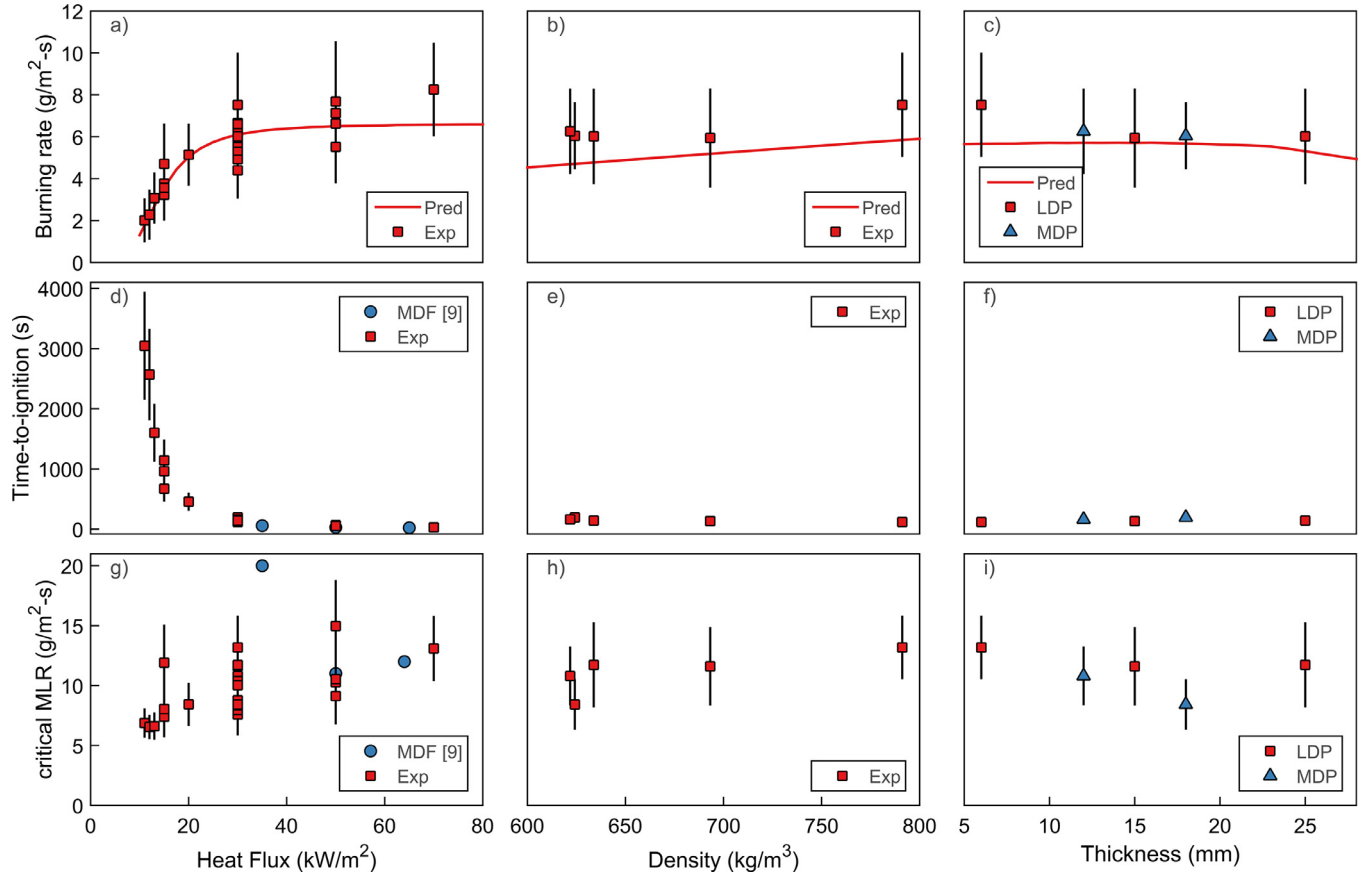

Fig. 11. Experimental and predicted data at different heat fluxes, density, and sample thickness. The average charring rate was determined from the full duration of the experiments. The dependency of the experimental duration against each variable was found from the experiments through correlations.LDP stands for low-density particleboard. MDP stands for medium-density particleboard.

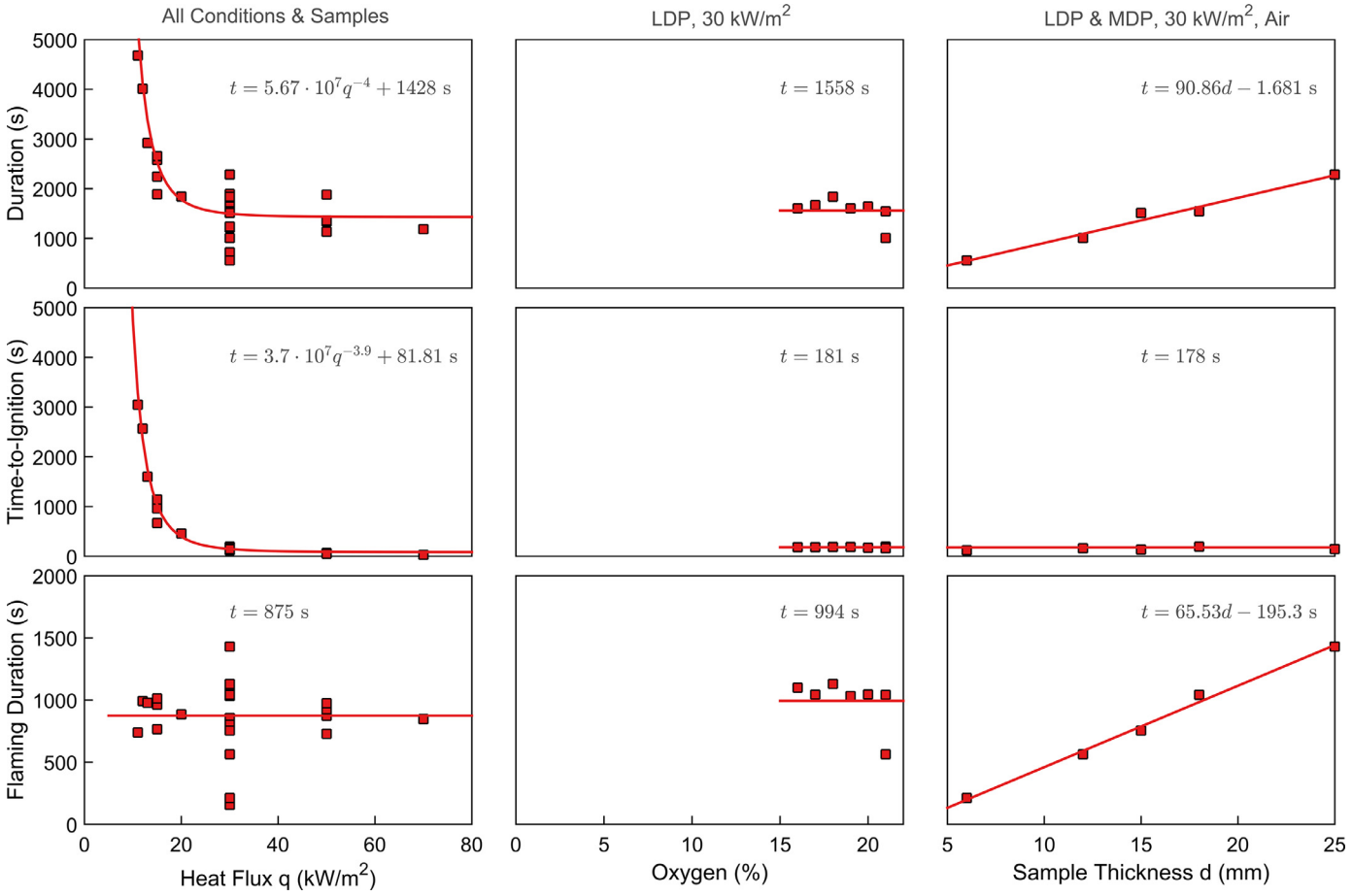

Fig. 12. The correlation between duration of the experiment, time-to-ignition, duration of flaming with heat flux, oxygen, and thickness used in the simulations are derived from the experimental measurements.

expected to vary with wood species and potentially experimental set-up. Near this triple point, a small change in the condition can result in either pyrolysis, flaming, or smouldering. We can further conclude that the fire risk near this triple point is disproportionately large to the expected risk. Crossing the smouldering ignition threshold near this triple point is likely to lead to an increase in heat flux from smouldering combustion. This additional heat could then cause the crossing of the flaming threshold, which means that near the triple point, the flaming threshold is effectively lower than anticipated when smouldering is neglected. This point highlights the importance of considering smouldering combustion as a fire safety hazard when dealing with wood e.g. in timber construction, wood storage, or wildfires. Smouldering combustion presents a danger in itself and a catalyst for flaming combustion.

3.4. Other influencing parameters

Fig. 11a & d show that the charring rate increases and time-to-ignition (flaming) decreases with heat flux[45]. The critical ignition heat flux for flaming ignition was found to be 10 kW/m^2 (Fig. 11a), and the critical mass loss rate was around 10 g/m^2-s (Fig. 11g) in air, which is in line with the literature [9,45]. The latter was found to be constant across different densities and thicknesses. Surprisingly, we found that density and sample thickness (Fig. 11b&c) did not affect the charring rate at 30 kW/m^2 in air. The model does predict a slight increase in charring rate with density (Fig. 11b), as would be expected, but such a trend is within the experimental errors. Thus, the density influence (1.6 g/m^2-s) is quite small, compared to the influence of heat flux (6.2 g/m^2-s) and does not affect the burning mode like oxygen. Similarly, the model predicts a slight decrease in the charring rate with an increase in sample thickness (Fig. 11c), meaning that all samples acted as thermally thick. Again, this influence (1 g/m^2-s) was small compared to the influence of oxygen concentration and heat flux. The fitting correlations used in the simulations for duration, time-to-ignition, and duration of flaming are summarised in Fig. 12. These findings imply that future experiments should continue to focus on heat flux and oxygen concentration.

This study has two potential limitations. The first limitation of our study is the extrapolation of our smouldering and flaming criticality. Hadden et al. [39] argued that the criticality of self-sustained smouldering is dependant on the fuel type, experimental set-up, and environmental variables. Subsequent studies, however, found different limiting oxygen concentrations (13.5% in [46] and 10% in [19]), meaning that the 4% limiting oxygen concentration for smouldering wood found by this study depends on the heat flux, scale, and other parameters. Another limitation is that we restricted ourselves to one kind of engineered wood material. However, all engineered woods are produced from natural wood and resin or glue. Therefore, their fundamental chemical composition and largely their microstructure should be similar so that our results should hold, at least qualitatively, for most engineered woods.

4. Conclusions

In this paper, we experimentally and computationally characterised the influence of oxygen concentration and other variables

on the burning behaviour of particleboard. Heat flux had a significant influence, while density and sample thickness had no effect on the charring rate and time-to-flaming ignition. Oxygen concentration controls the mode of burning with pyrolysis dominating below 4% $[O_2]_a$, smouldering between 4 and 15% $[O_2]_a$, and flaming above 15%. These thresholds agree with the literature. Comparing the mass loss rates at different oxygen concentrations revealed that flaming enhanced the mass loss rates by 37% compared to pure pyrolysis and smouldering. This finding led us to the hypothesis that smouldering can lead to significant additional strength-loss in structural timber after flaming has ceased. Simultaneously studying the effect of heat flux and oxygen concentration on the ignition thresholds for smouldering and flaming ignition of wood demonstrated that the limited minimum oxygen concentration required for ignition reduces with heat flux for both smouldering and flaming. For the first time, this analysis revealed a triple point for wood at which a small change in condition can lead to either smouldering, flaming, or pyrolysis. More importantly, smouldering increases the fire hazard of wood near the triple point by providing a low resistance route to flaming. Smouldering is currently not part of timber buildings' fire safety design and we recommend revisiting this assumption. Smouldering combustion presents a danger in itself and a catalyst for flaming combustion. In summary, our paper provides the criticalities for each mode of the burning of wood, the first step towards studying the transition between the three modes (pyrolysis, smouldering, flaming).

Declaration of Competing Interest

None.

Acknowledgment

The authors thank EPSRC, Arup, and BRE Trust for financial support and the University of Edinburgh for the experimental facilities used. Furthermore, we thank members of Imperial Hazelab for insightful discussions and helpful comments.

Supplementary materials

Supplementary material associated with this article can be found, in the online version, at doi:10.1016/j.combustflame.2021.111591.

References

[1] S. Deeny, R.M. Hadden, A. Lawrence, B. Lane, Fire safety design in modern timber buildings, Struct. Eng. 96 (2018) 48–53.
[2] W.C. Park, A. Atreya, H.R. Baum, Experimental and theoretical investigation of heat and mass transfer processes during wood pyrolysis, Combust. Flame. 157 (2010) 481–494.
[3] K. Li, X. Huang, C. Fleischmann, G. Rein, J. Ji, Pyrolysis of medium density fibreboard: optimized search for kinetic scheme and parameters via genetic algorithm driven by Kissinger's method, Energy & Fuels (2014) 140822231738003.
[4] D. Zeinali, S. Verstockt, T. Beji, G. Maragkos, J. Degroote, B. Merci, Experimental study of corner fires—part II: flame spread over MDF panels, Combust. Flame. 189 (2018) 491–505.
[5] R.S. Miller, J. Bellan, A generalized biomass pyrolysis model based on superimposed cellulose, hemicellulos eand liqnin kinetics, Combust. Sci. Technol. 126 (1997) 97–137.
[6] G. Argawal, M. Chaos, Y. Wang, D. Zeinali, Pyrolysis model properties of engineered wood products and validaton using transient heating scenarios, Interflam (2016).
[7] K. Li, S. Hostikka, P. Dai, Y. Li, H. Zhang, J. Ji, Charring shrinkage and cracking of fir during pyrolysis in an inert atmosphere and at different ambient pressures, Proc. Combust. Inst. (2016) 1–10 000.
[8] N. Boonmee, J.G. Quintiere, Glowing and flaming autoignition of wood, Proc. Combust. Inst. 29 (2002) 289–296.
[9] X. Huang, K. Li, H. Zhang, Modelling bench-scale fire on engineered wood: effects of transient flame and physicochemical properties, Proc. Combust. Inst. 36 (2017) 3167–3175.
[10] J. Schmid, A. Santomaso, D. Brandon, U. Wickström, A. Frangi, Timber under real fire conditions – the influence of oxygen content and gas velocity on the charring behavior, World Conf. Timber Eng, 2016.
[11] T.J. Ohlemiller, Forced smolder propagation and the transition to flaming in cellulosic insulation, Combust. Flame. 81 (1990) 354–365.
[12] G. Rein, Smoldering Combustion, SFPE Handb. Fire Prot. Eng., Springer, New York, New York, NY (2016), pp. 581–603.
[13] X. Huang, J. Gao, A review of near-limit opposed fire spread, Fire Saf. J. 120 (2021) 103141.
[14] R. Crielaard, J.W. van de Kuilen, K. Terwel, G. Ravenshorst, P. Steenbakkers, Self--extinguishment of cross-laminated timber, Fire Saf. J. 105 (2019) 244–260.
[15] R. Emberley, T. Do, J. Yim, J.L. Torero, Critical heat flux and mass loss rate for extinction of flaming combustion of timber, Fire Saf. J. (2017) 1.
[16] D.J. Rasbash, B. Langford, Burning of wood in atmospheres of reduced oxygen concentration, Combust. Flame. 12 (1968) 33–40.
[17] C.M. Belcher, J.C. McElwain, Limits for combustion in low O_2 redefine paleoatmospheric predictions for the mesozoic, Science 321 (80) (2008) 1197–1200.
[18] J. Cuevas, J.L. Torero, C. Maluk, Flame extinction and burning behaviour of timber under varied oxygen concentrations, Fire Saf. J. (2020) 23.
[19] H. Wang, P.J. Van Eyk, P.R. Medwell, C.H. Birzer, Z.F. Tian, M. Possell, Effects of oxygen concentration on radiation-aided and self-sustained smoldering combustion of radiata pine, Energy and Fuels 31 (2017) 8619–8630.
[20] D. Morrisset, R.M. Hadden, A.I. Bartlett, A. Law, R. Emberley, Time dependent contributions of char oxidation and flame heat feedback on the mass loss rate of timber, Fire Saf. Sci. Proc. Thirteen. Int. Symp. (2020) 103058.
[21] F.X.J. Calle, Application of Fire Calorimetry to Understand Factors Affecting Flammability of Cellulosic material: Pine needles, Tree Leaves and Chipboard, 2012.
[22] C. Lautenberger, C. Fernandez-Pello, A model for the oxidative pyrolysis of wood, Combust. Flame. 156 (2009) 1503–1513.
[23] F. Richter, G. Rein, Heterogeneous kinetics of timber charring at the microscale, J. Anal. Appl. Pyrolysis. 138 (2019) 1–9.
[24] F. Richter, G. Rein, A multiscale model of wood pyrolysis in fire to study the roles of chemistry and heat transfer at the mesoscale, Combust. Flame. 216 (2020) 316–325.
[25] F. Richter, P. Kotsovinos, E. Rackauskaite, G. Rein, Thermal response of timber slabs exposed to travelling fires and traditional design fires, Fire Technol (2020).
[26] T. Kashiwagi, H. Nambu, Global kinetic constants for thermal oxidative degradation of a cellulosic paper, Combust. Flame. 88 (1992) 345–368.
[27] T.J. Ohlemiller, Smoldering combustion propagation through a permeable horizontal fuel layer, Combust. Flame. 81 (1990) 341–353.
[28] A. Anca-Couce, N. Zobel, A. Berger, F. Behrendt, Smouldering of pine wood: kinetics and reaction heats, Combust. Flame. 159 (2012) 1708–1719.
[29] F. Richter, A. Atreya, P. Kotsovinos, G. Rein, The effect of chemical composition on the charring of wood across scales, Proc. Combust. Inst. 37 (2019) 4053–4061.
[30] X. Huang, G. Rein, Thermochemical conversion of biomass in smouldering combustion across scales: the roles of heterogeneous kinetics, oxygen and transport phenomena, Bioresour. Technol. 207 (2016) 409–421.
[31] T. Kashiwagi, T.J. Ohlemiller, K. Werner, Effects of external radiant flux and ambient oxygen concentration on nonflaming gasification rates and evolved products of white pine, Combust. Flame. 69 (1987) 331–345.
[32] G. Wu, D.U. Shah, E.R. Janeček, H.C. Burridge, T.P.S. Reynolds, P.H. Fleming, P.F. Linden, M.H. Ramage, O.A. Scherman, Predicting the pore-filling ratio in lumen-impregnated wood, Wood Sci. Technol. 51 (2017) 1277–1290.
[33] X. Huang, G. Rein, H. Chen, Computational smoldering combustion: predicting the roles of moisture and inert contents in peat wildfires, Proc. Combust. Inst. 35 (2015) 2673–2681.
[34] M. Zarzecki, J.G. Quintiere, R.E. Lyon, T. Rossmann, F.J. Diez, The effect of pressure and oxygen concentration on the combustion of PMMA, Combust. Flame. 160 (2013) 1519–1530.
[35] D.E. Ward, C.C. Hardy, Smoke emissions from wildland fires, Environ. Int. 17 (1991) 117–134.
[36] W.C. Park, A. Atreya, H.R. Baum, Determination of pyrolysis temperature for charring materials, Proc. Combust. Inst. 32 (2009) 2471–2479.
[37] T.J. Ohlemiller, Modeling of smoldering combustion propagation, Prog. Energy Combust. Sci. 11 (1985) 277–310.
[38] M.G. Ortiz-Molina, T.Y. Toong, N.A. Moussa, G.C. Tesoro, Smoldering combustion of flexible polyurethane foams and its transition to flaming or extinguishment, Symp. Combust. 17 (1979) 1191–1200.
[39] R.M. Hadden, G. Rein, C.M. Belcher, Study of the competing chemical reactions in the initiation and spread of smouldering combustion in peat, Proc. Combust. Inst. 34 (2013) 2547–2553.
[40] A.I. Bartlett, R.M. Hadden, L.A. Bisby, A review of factors affecting the burning behaviour of wood for application to tall timber construction, Fire Technol 55 (2019) 1–49.
[41] F. Wiesner, L.A. Bisby, A.I. Bartlett, J.P. Hidalgo, S. Santamaria, S. Deeny, R.M. Hadden, Structural capacity in fire of laminated timber elements in compartments with exposed timber surfaces, Eng. Struct. 179 (2019) 284–295.
[42] H. Kinjo, Y. Katakura, T. Hirashima, S. Yusa, K. Saito, Deflection behavior and load-bearing period of structural glued laminated timber beams in fire including cooling phase, J. Struct. Fire Eng. 9 (2018) 287–299.
[43] A. Bartlett, F. Wiesner, R. Hadden, L. Bisby, B. Lane, A. Lawrence, P. Palma, A. Frangi, Needs for total fire engineering of mass timber buildings, WCTE 2016 - World Conf. Timber Eng, 2016.

[44] K. Miyamoto, X. Huang, N. Hashimoto, O. Fujita, C. Fernandez-Pello, Limiting oxygen concentration (LOC) of burning polyethylene insulated wires under external radiation, Fire Saf, J. 86 (2016) 32–40.
[45] N. Bal, Forty years of material flammability: an appraisal of its role, its experimental determination and its modelling, Fire Saf. J. 96 (2018) 46–58.
[46] J. Yang, N. Liu, H. Chen, W. Gao, R. Tu, Effects of atmospheric oxygen on horizontal peat smoldering fires: experimental and numerical study, Proc. Combust. Inst. 37 (2019) 4063–4071.
[47] S. Lin, X. Huang, J. Gao, J. Ji, Extinction of Wood Fire: A Near-Limit Blue Flame Above Hot Smoldering Surface, Fire Technology (2021) In press.